Journal of Alloys and Compounds 509S (2011) S595–S598

Contents lists available at ScienceDirect

Journal of Alloys and Compounds

journal homepage: www.elsevier.com/locate/jallcom

Hydrogen sorption properties of a MgH_2–10 wt.% graphite mixture

F.J. Castro [a,b,*], V. Fuster [a,b], G. Urretavizcaya [a,b]

[a] Centro Atómico Bariloche (CNEA, CONICET), R8402AGP, S.C. de Bariloche, Río Negro, Argentina
[b] Instituto Balseiro (UNCuyo, CNEA), R8402AGP, S.C. de Bariloche, Río Negro, Argentina

ARTICLE INFO

Article history:
Received 29 October 2010
Received in revised form 5 January 2011
Accepted 7 January 2011
Available online 15 January 2011

Keywords:
Hydrogen storage
Hydrides
Sorption kinetics
Magnesium
Mechanical milling

ABSTRACT

We present an analysis of the hydrogen absorption and desorption properties of a MgH_2–10 wt.% graphite mixture prepared by reactive mechanical milling. The analysis is based on isothermal hydriding and dehydriding kinetic measurements and calorimetry experiments. The studied samples contained different hydrogen contents. From the characteristics of the sorption curves several features of the hydriding and dehydriding processes are identified. Additionally, the role of graphite in hydrogen sorption is analyzed.

1. Introduction

Hydrogen storage in Mg based materials has been extensively studied due to magnesium's low cost and high theoretical hydrogen storage capacity [1,2]. One aspect of these materials considerably investigated is hydrogen sorption kinetics, one of the limitations to the widespread use of Mg [1,2]. Despite the efforts made, no consensus has been reached on the rate limiting steps on hydrogen absorption and desorption in Mg and Mg based materials. Absorption and desorption rates have been found to be controlled by nucleation and growth mechanisms, by the surface, by diffusion or by the interphase reaction [3–11]. Additionally, though several papers have shown that carbon and carbon allotropes have a beneficial effect on hydrogen sorption in Mg [12–21], the role that carbon plays in these processes has not yet been clearly established.

The purpose of this short paper is to contribute to the understanding of the hydrogen sorption process in Mg–C compounds. We focus on hydrogen absorption and desorption on a MgH_2–10 wt.% graphite mixture obtained by reactive mechanical milling. The study is based on isothermal hydriding and dehydriding kinetic measurements and on non-isothermal differential scanning calorimetry (DSC) results, both on partially hydrided samples.

2. Experimental

The MgH_2–C (graphite) mixture has been prepared by reactive mechanical milling Mg powder (99%, Riedel de Haën) and 10 wt.% C powder (Aldrich) for 80 h under 500 kPa of H_2 in a Uni-Ball-Mill II (Australian Scientific Instruments) apparatus. The hydrogen content of the final material was 6.1 wt.% (90% of the theoretical value). The synthesis process and the microstructural evolution of the mixture was similar to the one reported in [18]. Partially hydrided samples were extracted from the milling chamber during synthesis and their desorption properties studied by DSC in a TA DSC 2910 Instrument under flowing Ar. The 80 h milled material was also studied by isothermal (300 °C) hydriding and dehydriding kinetic measurements with different hydrogen contents in a custom made Sieverts type volumetric device. Desorption was measured on partially hydrided samples obtained by exposing a fully desorbed sample to 1000 kPa of H_2 at 300 °C during controlled time intervals (loading times). Analogously, absorption experiments were carried out on partially dehydrided samples obtained by desorbing a fully hydrided sample under 30 kPa of H_2 at 300 °C during controlled unloading times. Desorption and absorption experiments were started immediately after the loading and unloading times and performed under 30 kPa and 800 kPa of H_2, respectively. The reported measurements were obtained after performing several hydriding and dehydriding cycles until the curves showed full repeatability.

3. Results and discussion

The XRD pattern of the as-milled MgH_2–C mixture (Fig. 1A) presents reflections corresponding to β-MgH_2 (JCPDS card 12-0697), γ-MgH_2 (JCPDS card 35-1184), unreacted Mg (JCPDS card 35-0821), and a small peak of MgO (JCPDS card 45-0946). The appearance of the high-pressure γ-MgH_2 is a consequence of the milling process [22]. No C reflections can be identified, probably due to C amorphization during milling [19,20]. The XRD pattern of the same material after several hydriding and dehydriding cycles (Fig. 1B) only presents the reflections of β-MgH_2 and a small peak

* Corresponding author at: Centro Atómico Bariloche (CNEA, CONICET), R8402AGP, S.C. de Bariloche, Río Negro, Argentina. Tel.: +54 2944 445100; fax: +54 2944 445199.
E-mail address: fcastro@cab.cnea.gov.ar (F.J. Castro).

0925-8388/$ – see front matter © 2011 Elsevier B.V. All rights reserved.
doi:10.1016/j.jallcom.2011.01.069

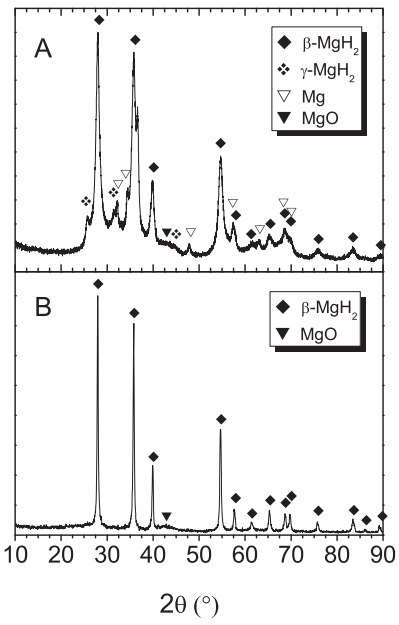

Fig. 1. XRD patterns of the MgH_2–C mixture. (A) As milled and (B) after hydrogen cycling.

of MgO. As a consequence of hydrogen cycling, β-MgH_2 crystallite size grows from 5 nm to 28 nm, as estimated with the Scherrer equation.

The MgH_2–C mixture presents much better sorption characteristics than MgH_2 without additives (Fig. 2). As both materials present similar microstructures acquired by mechanical milling [18], the differences can be attributed to the presence of C. To investigate the C role, isothermal absorption and desorption curves with different hydrogen initial contents were measured for the MgH_2–C mixture. Desorption curves present a shape that depends on the previous hydrogen loading (Fig. 3A). For hydrogen contents up to 4.5 wt.% desorption is practically linear, whereas above this value the desorption curves gradually become sigmoidal. Additionally, the higher initial desorption rates occur for the lower starting hydrogen content. This feature is also present in the complete desorption curve (the desorption curve of the fully hydrided sample). There desorption rates increase as the amount of hydrogen in the sample diminishes. However, the initial rates for the partially loaded samples do not coincide with the rates observed in the complete desorption curve at the same hydrogen contents (Fig. 3A, inset). That is, desorption curves of the partially hydrided samples are not just time-translated pieces of the complete desorption curve. These results suggest that desorption kinetics is controlled by different processes. On the one hand, the sigmoidal shape of the desorption curve of the fully hydrided sample implies that desorption is controlled by a nucleation and growth process. On the other hand, the linear shape of the partially hydrided desorption curves suggests a surface controlled desorption process. These differences can be explained by the coexistence of Mg and MgH_2 in each desorbing particle for global hydrogen contents below 4.5 wt.% [10,11,23]. Following the ideas presented for MgH_2 without additives in [10,11], the observed behavior can be rationalized by considering that the incompletely hydrided samples contain Mg islands that grow during dehydriding and make metal nucleation unnecessary. Additionally, these islands provide a preferential desorption path that permits the H surface recombination to become the rate limiting process. In the case of the fully hydrided sample, no Mg islands are available from the start, and hence desorption must proceed by a nucleation and growth mechanism. The partially hydrided samples with hydrogen content between 4.5 wt.% and 6 wt.% constitute an intermediate case, where some particles contain both Mg and MgH_2 and some others only MgH_2. Then, desorption curves gradually loose their linear shape and become sigmoidal as hydrogen loading grows.

It remains to be explained why the initial desorption rates of the partially hydrided samples do not coincide with the initial rates of the completely hydrided sample (Fig. 3A, inset). This fact can be understood taking into account the spatial distribution of the hydride in these materials. The coexistence of Mg and MgH_2 implies that hydriding proceeds by the formation and growth of hydride nuclei. Thus, considering how the partially hydrided samples were obtained it can be assumed that the hydride is preferentially located near the surface (see schemes in Fig. 3) and [10]. In contrast, at intermediate stages of the complete desorption curve the hydride is mainly located near the centre of the particles, due to the fact that the material was fully hydrided at the beginning and desorption proceeds by the growth of Mg nuclei formed on the surface [10]. Therefore, in this last case the hydrogen atoms must diffuse through the Mg matrix to reach the surface, whereas in the partially hydrided samples the hydrogen atoms can get to the surface much faster by diffusing along the Mg/MgH_2 interphase. This faster diffusion process provides an explanation for the observed higher rates and also makes possible a surface controlled process.

Hydrogen desorption from the partially hydrided samples obtained at intermediate milling stages was characterized by DSC (Fig. 4). The striking feature is the displacement of the desorption peaks towards higher temperatures as milling time (and hydrogen content) increase. That is, desorption kinetics seems to get worse with milling time. This is somewhat surprising, because as milling proceeds kinetics is expected to improve due to microstructural refinement. However, the similarity between this shift and the lowering rates observed in Fig. 3A suggests that peak relocation could

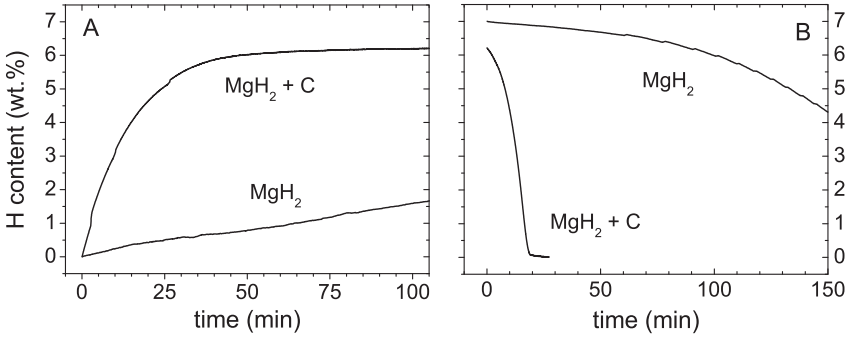

Fig. 2. Isothermal hydrogen absorption and desorption in the MgH_2–C mixture and MgH_2 without additive. (A) Absorption at 200 °C under 1000 kPa of H_2 and (B) desorption at 300 °C under 30 kPa of H_2.

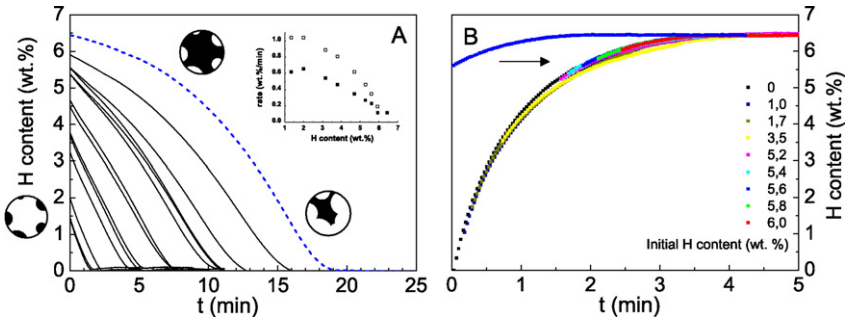

Fig. 3. (A) Hydrogen desorption with different hydrogen initial contents at 300 °C and 30 kPa of H_2. The blue dashed desorption curve correspond to the fully hydrided sample. The inset shows the hydrogen desorption rate as a function of hydrogen content. The filled symbols correspond to different stages of the fully hydrided material; the empty symbols correspond to the initial rate of the partially hydrided samples. The schemes illustrate the spatial distribution of hydride (black) on a particle. (B) Hydrogen absorption at 300 °C and 800 kPa of H_2 with different initial hydrogen contents (indicated in the figure). The curves have been time translated, as indicated by the blue curve. (For interpretation of the references to color in this figure legend, the reader is referred to the web version of the article.)

be a consequence of a desorption process controlled by the surface. To verify this, we plotted together the DSC curves of the 20 h, 28 h, 36 h and 80 h milled materials (Fig. 4, inset). We observe that the DSC curves of the partially hydrided materials have a common onset and coincide in the ascending part of the peak. On the contrary, the DSC curve of the 80 h milled material does not belong to this group as it is clearly shifted to the right. The coincidence in the ascending part of several desorption peaks and the shift of the maxima with increasing hydrogen contents is an exclusive characteristic of a surface controlled process [11]. As an additional evidence of this, we observe that the temperature dependence of the ascending part of the peaks agrees quite well with the expected Arrhenius type temperature dependence of a surface controlled process [11]. From this temperature dependence, we calculated an activation energy of 134 kJ/mol. Therefore, it can be assumed again that at intermediate milling stages the milled particles contain a mixture of Mg and MgH_2 (preferentially located near the surface) and desorption is controlled by the surface recombination of two H atoms. In the case of the 80 h milled material, the absence of Mg islands on the surface makes the nucleation step unavoidable, and as a result desorption is delayed towards higher temperatures.

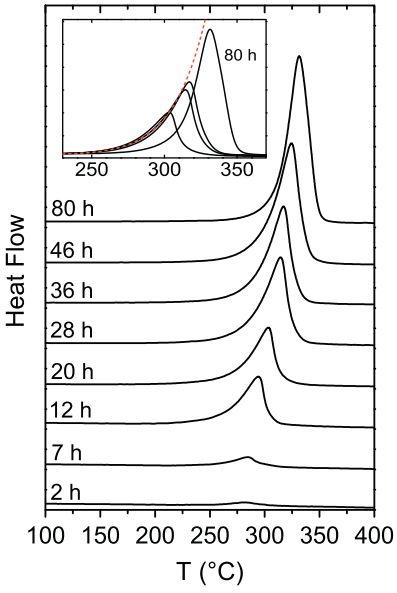

Fig. 4. DSC thermograms for different milling times. The area under the curves is proportional to the hydrogen content. The inset shows the thermograms of the samples milled (from left to right) 20 h, 28 h, 36 h and 80 h. The dotted red line indicates the fit of the ascending part of the peak with an Arrhenius function. (For interpretation of the references to color in this figure legend, the reader is referred to the web version of the article.)

Therefore, though graphite greatly improves hydrogen desorption kinetics, the rate limiting mechanism coincides with the controlling steps reported for MgH_2 without additives [11,23–25]. Thus, the role of C seems to be to increase the rate of the controlling steps without changing them. In the case of the partially hydrided samples it favors the surface processes, and in the case of the fully hydrided sample it enhances nucleation.

The isothermal hydrogen absorption curves do not present as many features as the desorption ones. In Fig. 3B we see that the absorption curves of the partially dehydrided samples coincide quite well with the total absorption curve if they are appropriately time-translated. From this agreement we conclude that a uniform hydride layer completely surrounding the particles is not formed during hydriding. If this were the case, the intermediate hydriding stages of the complete absorption curve (mostly surrounded by MgH_2) would be much slower than the hydrogen absorption in the previously partially dehydrided samples (mostly surrounded by Mg), due to the differences in H diffusion in Mg and MgH_2 [26]. The formation of a uniform hydride layer surrounding the Mg particles has been reported for non-milled Mg [27]. The absence of this layer can be due either to a nucleation process on the surface with a reduced number of nuclei, or to a nucleation step not restricted to the surface of the material (possibly with C acting as a nucleation centre).

4. Conclusion

Hydrogen sorption kinetics in a MgH_2 + 10 wt.% graphite mixture prepared by reactive mechanical milling was studied by isothermal volumetric experiments and non-isothermal DSC measurements. The sorption processes have been analyzed for different hydrogen contents. Hydrogen desorption was found to be a nucleation and growth controlled process that can change to a surface controlled process when hydrogen desorbs from partially hydrided samples due to the coexistence of Mg and MgH_2 in the desorbing particles. In this last case, Mg islands make the nucleation step unnecessary and provide a more favorable desorption path. Graphite does not change the controlling step during desorption reported for MgH_2 without additives, it favors Mg nucleation and accelerates the processes that occur on the surface during hydrogen desorption. Hydrogen absorption was found to proceed without the formation of a uniform hydride layer surrounding the Mg particles. This can be due to a nucleation process not restricted to the surface of the material or to a nucleation step proceeding with the formation of a reduced number of MgH_2 nuclei.

Acknowledgments

The authors gratefully acknowledge partial financial support from FONCyT PICT No. 821 and PAE-PICT No. 133, and from Universidad Nacional de Cuyo.

References

[1] I.P. Jain, C. Lal, A. Jain, Int. J. Hydrogen Energy 35 (2010) 5133–5144.
[2] L. Schlapbach, A. Zuttel, Nature 414 (2001) 353.
[3] J.S. Han, M. Pezat, J.-Y. Lee, J. Less-Common Metals 130 (1987) 395–402.
[4] J.R. Fernández, C.R. Sánchez, J. Alloys Compd. 340 (2002) 189–198.
[5] G. Barkhordarian, T. Klassen, R. Bormann, J. Alloys Compd. 407 (2006) 249–255.
[6] H.Y. Tien, M. Tanniru, C.-Y. Wu, F. Ebrahimi, Int. J. Hydrogen Energy 34 (2009) 6343–6349.
[7] L. Pasquini, E. Callini, E. Piscopiello, A. Montone, M. Vittori Antisari, E. Bonetti, Appl. Phys. Lett. 94 (2009) 41918.
[8] J.R. Ares, F. Leardini, P. Díaz-Chao, J. Bodega, D.W. Koon, I.J. Ferrer, J.F. Fernández, C. Sánchez, J. Alloys Compd. 495 (2010) 650–654.
[9] A. Montone, A. Aurora, D. Mirabile Gattia, M. Vittori Antisari, Scripta Mater. 63 (2010) 456–459.
[10] M. Tanniru, H.-Y. Tien, F. Ebrahimi, Scripta Mater. 63 (2010) 58–60.
[11] E. Evard, I. Gabis, V.A. Yartys, Int. J. Hydrogen Energy 35 (2010) 9060–9069.
[12] S. Dal Toè, S. Lo Russo, A. Maddalena, G. Principi, A. Saber, S. Sartori, T. Spataru, Mater. Sci. Eng. B108 (2004) 24–27.
[13] S. Bouaricha, J.-P. Dodelet, D. Guay, J. Mater. Res. 16 (2001) 2893–2905.
[14] J. Huot, M.-L. Tremblay, R. Schulz, J. Alloys Compd. 356–357 (2003) 603–607.
[15] C.X. Shang, Z.X. Guo, J. Power Sources 129 (2004) 73–80.
[16] Z.G. Huang, Z.P. Guo, A. Calka, D. Wexler, J. Wu, P.H.L. Notten, H.K. Liu, Mater. Sci. Eng. A 447 (2007) 180–185.
[17] M.A. Lillo-Ródenas, Z.X. Guo, K.F. Aguey-Zinsou, D. Cazorla-Amorós, Carbon 46 (2008) 126–137.
[18] V. Fuster, G. Urretavizcaya, F.J. Castro, J. Alloys Compd. 481 (2009) 673–680.
[19] H. Imamura, N. Sakasai, J. Alloys Compd. 231 (1995) 810–814.
[20] H. Imamura, Y. Takesue, T. Akimoto, S. Tabata, J. Alloys Compd. 293–295 (1999) 564–568.
[21] H. Imamura, S. Tabata, N. Shigetomi, Y. Takesue, Y. Sakata, J. Alloys Compd. 330–332 (2002) 579–583.
[22] F. Gennari, F. Castro, G. Urretavizcaya, J. Alloys Compd. 321 (2001) 46–50.
[23] K.B. Gerasimov, I.G. Konstanchuck, S.A. Chizhik, J.-L. Bobet, Int. J. Hydrogen Energy 34 (2009) 1916–1921.
[24] K.B. Gerasimov, E. Yu Ivanov, Mater. Lett. 3 (1985) 497–499.
[25] K. Gerasimov, I. Konstanchuk, J.-L. Bobet, Ann. Chim. Sci. Mater. 34 (2009) 391–399.
[26] J. Topler, H. Buchner, H. Saufferer, J. Less-Common Metals 88 (1982) 397–404.
[27] G. Friedlmeier, M. Groll, J. Alloys Compd. 253–254 (1997) 550–555.